Estimation of Dielectric Concrete Properties from Power Measurements at 18.7 and 60 GHz

Bruno Feitor[#1], Rafael Caldeirinha[#*2], Telmo Fernandes[#*3], David Ferreira[#4], Nuno Leonor[#5]

#Polytechnic Institute of Leiria, ESTG and Institute of Telecommunications - DL
Alto do Vieiro – Leiria, Portugal

[1]2080430@my.ipleiria.pt
[2]rafael.caldeirinha@ ipleiria.pt
[3]telmo.fernandes@ipleiria.pt
[4]david.ferreira@co.it.pt
[5]2101533@my.ipleiria.pt

**University of Glamorgan, Faculty of Advanced Technology*
CF 37 1DL Treforest, United Kingdom

***Abstract*— In this paper, microwave and millimetre wave reflection coefficient measurements at 18.7 and 60 GHz are presented for a group of concrete slabs, in which only the thickness of the gravel present inside is varied. An empirical reflection coefficient value is determined using both reflected and LOS power measurements. A concrete slab with no gravel is used as a reference. The measurement results show the dependence of the reflection coefficient with the thickness of the gravel inside the slab. The measurement results allow for the appropriate extraction of dielectric properties of the materials under study.**

I. INTRODUCTION

The demand for higher data rates in indoor wireless communications is growing at a fast pace. Current communication systems operate at speeds of a few Mbps in the ISM band at 2.4GHz. However, higher data rates will require larger bandwidths and consequently higher carrier frequencies. This increase in frequency may lead to different propagation characteristics depending on the medium type.

Therefore, it is necessary to understand the reflection and transmission characteristics of common building materials, such as concrete walls, in order to model the propagation behaviour of indoor radio systems. Although similar studies can be found in literature [1-3], current work is focused on the phenomena of reflection in various types of concrete. To this extent, the reflection losses of concrete structures have been characterised at frequencies of 18.7 and 60 GHz when different sizes of gravel are used in its composition.

II. REFLECTION MODELS

Assuming an incident electric field with a planar waveform and constant phase, the Fresnel reflection coefficients (ρ) relate both the incident and the reflected fields from an infinite dielectric slab. The Fresnel reflection coefficients [4] are given by (1) and (2), respectively, for TM and TE polarisations.

$$\rho_{TM} = \frac{\sqrt{\left(\frac{n'}{n}\right)^2 - \sin^2(\theta)} - \left(\frac{n'}{n}\right)^2 \cos(\theta)}{\sqrt{\left(\frac{n'}{n}\right)^2 - \sin^2(\theta)} + \left(\frac{n'}{n}\right)^2 \cos(\theta)} \quad (1)$$

$$\rho_{TE} = \frac{\cos(\theta) - \sqrt{\left(\frac{n'}{n}\right)^2 - \sin^2(\theta)}}{\cos(\theta) + \sqrt{\left(\frac{n'}{n}\right)^2 - \sin^2(\theta)}} \quad (2)$$

where n is the complex refractive index which depends on the dielectric material properties, n' represents the refractive index of the air and θ expresses the incidence angle with respect to a vector normal to the surface [5].

The Fresnel reflection model assumes an infinite dielectric slab. However, multi-dielectric structures are often used in building. Therefore, and for these particular cases, a multi-dielectric model, which must take into account many slabs of different materials with different thicknesses, is required. Such model is given by (3), representing the reflection coefficient of the multi-dielectric model, which depends on the elementary reflection coefficients and phase thicknesses presented in (4).

$$\Gamma_i = \frac{\rho_i + \Gamma_{i+1} e^{-2j\delta_i}}{\rho_i - \Gamma_{i+1} e^{-2j\delta_i}} \quad \text{, i=a, 1, 2, ...M, b} \quad (3)$$

$$\delta_i = \frac{2\pi d_i}{\lambda} \sqrt{n_i^2 - n_a^2 \sin^2 \theta_a} \quad \text{, i=1, 2, …M} \quad (4)$$

The multilayer model admits multiple internal reflections in multilayer dielectric structures such as the one shown in Fig. 1.

978-1-4577-1016-2/11/$26.00 ©2011 IEEE

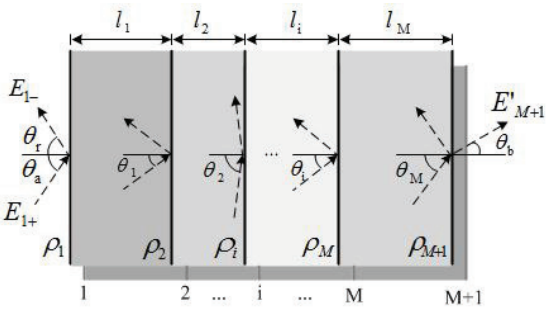

Fig. 1 – Oblique incidence in multilayer dielectric structure.

III. MEASUREMENT EQUIPMENT AND GEOMETRY

A. RF System

Continuous Wave (CW) measurements were conducted at the 18.7 and 60 GHz spot frequencies. The transmitter side of the 18.7 GHz measurement system, illustrated in Fig. 2, consisted of a 18.7 GHz PLL oscillator attached to a 20dBi gaussian horn antenna. The receiver consisted of a 20dBi standard horn antenna connected to a 38 dB low noise amplifier, which was in turn connected to a frequency mixer. This mixer is used to down-convert the received signal to a 500 MHz IF stage, and the corresponding power level was then measured utilising a spectrum analyser. This 18.7GHz system allowed measurements with a dynamic range for excess loss of approximately 80dB.

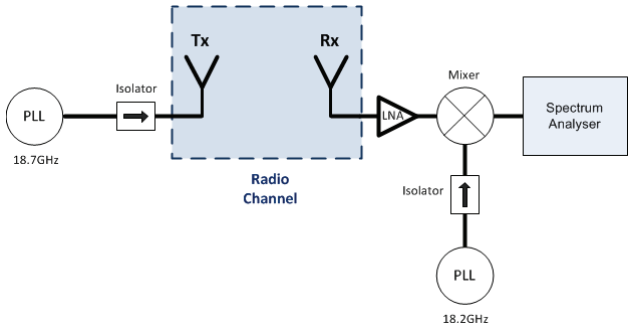

Fig. 2 – Block diagram of the 18.7GHz RF measurement system.

The 60 GHz measurement system transmitter, shown in Fig. 3, is similar to its 18.7 GHz counterpart, consisting of a 15GHz PLL oscillator connected to a multiplier (by 4), resulting in a 60 GHz CW signal. This signal passes through an isolator and enters the up-converter mixer, which also receives a 2 GHz IF signal derived from a signal generator. The modulated signal is then fed to a 25 dBi standard horn antenna. On the receiver side, the signal is acquired by an identical 25 dBi standard horn antenna, after which it is amplified by a LNA with 28 dB of gain. The RF signal is down-converted to IF by a 54 GHz LO signal (which results from a x4 multiplication of a 13.5GHz PLL signal). From the three spectrum components present at IF band, the spectrum analyser is configured to measure the power level from the IF-component present at 4GHz. Both PLLs of the 60GHz system, as well as the signal generator are kept synchronised by a 10 MHz reference signal from the spectrum analyser.

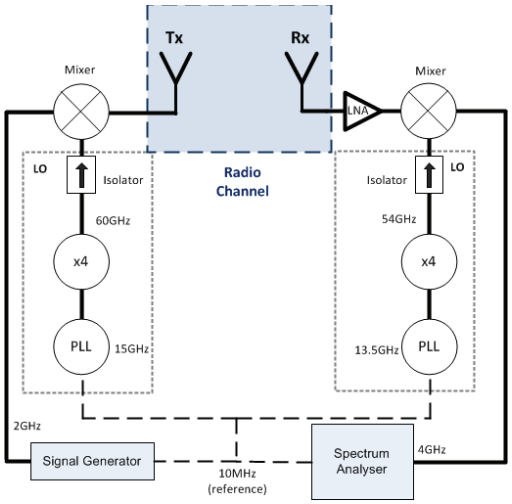

Fig. 3 – Block diagram of the 60GHz RF system.

B. Measurements methodology

Measurements were performed in order to characterise the reflection phenomena in slabs formed from various types of concrete. Such measurements were carried out in a controlled environment inside an anechoic chamber, in order to minimise interferences from unwanted signals and reflections. As shown in Fig. 4, the transmitter is in a fixed position while the receiver rotates in an arc around the slab under test in the angular range of 0 to 166º, in 1º steps. At the centre of the setup, the wall turns around its vertical axes from 0 to 90º, in 1º steps. For each angular step of the arm, the wall performs a full rotation within the specified limits. Due to physical constraints of the setup inside the anechoic chamber, namely the 180º position of the arm corresponding to the receiver being exactly in front of the transmitter, the arm rotation was limited to the aforementioned 166º.

C. Reflection coefficient measurement

Fig. 5 shows the reflection coefficient experiment performed using a two measurement technique [6]. The LOS measurement provides a reference for comparison with the power level from the reflection measurement.

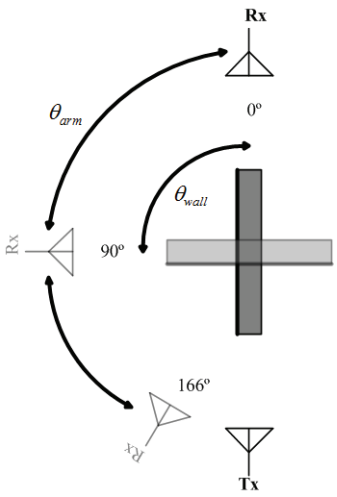

Fig. 4 - Measurement geometry

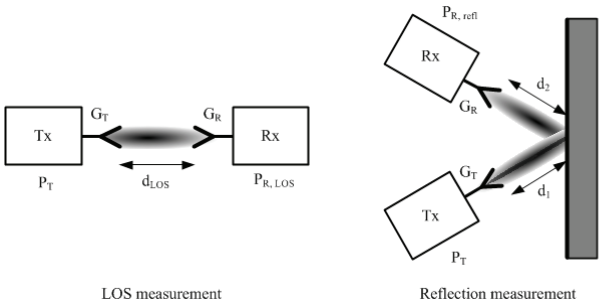

Fig. 5 – Two-measurement technique for reflection coefficient determination.

The LOS power level is taken to be the one given by the *Friis* transmission value [7], while the measured reflected power is taken to be the free space value for the unfolded path length times the reflection coefficient, as show in Eq. 5.

$$P_{R,refl} = \frac{P_T G_T G_R \lambda^2}{(4\pi)^2 (d_1 + d_2)^2} |\Gamma|^2 \quad (5)$$

Implicitly, (5) assumes that the reflecting boundary is infinitely large, which is approximately true when the wall dimensions are much larger than distances d_1 and d_2 and the wall surface area is much larger than the illuminated area [7]. Assuming these conditions are met, the ratio between (5), and the power level given by the *Friis* transmission formula of the LOS measurement, results in (6).

$$|\Gamma| = \frac{d_1 + d_2}{d_{LOS}} \sqrt{\frac{P_{R,refl}}{P_{R,LOS}}} \quad (6)$$

Thus, the empirical reflection coefficient is determined by the ratio of reflected and LOS power measurements, multiplying by the difference in measurement distances [7].

IV. Results and Analisys

This section is concerned with the comparison of the measured reflection coefficient from concrete walls slabs, compared to the predicted values using the multi-dielectric model. Measurements were made only in vertical polarisation.

All measurement results are compared to the multi-dielectric reflection formulae for smooth surfaces. Both the permittivity and loss tangent are found by fitting the measured values to theoretical predictions using the Root Mean Square Error (RMSE) minimisation criteria.

The 18.7 GHz measurement results are depicted in Figs 6 to 9 for the types of concrete in study. In these figures, it is possible to observe a relatively good agreement between measured and predicted results. These results show the reflection coefficient dependence with the thickness of the gravel inside the slabs. It is important to notice that the reflection coefficient increases with the increase of the gravel thickness.

Results obtained from measurements at 60 GHz are given in Figures 10 to 13, where both predicted and measured values are also in good agreement.

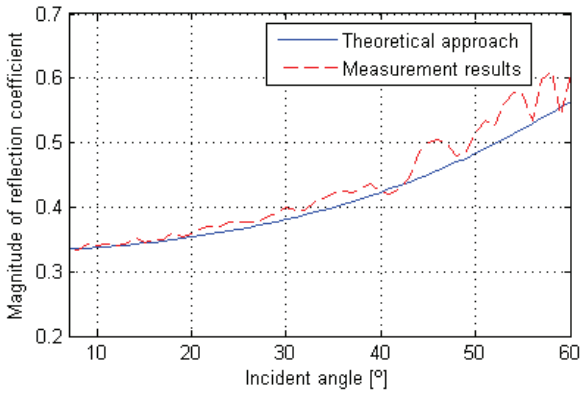

Fig. 6 – Measured and predicted reflection coefficient as function of incident angle for concrete slab without gravel, at 18.7GHz.

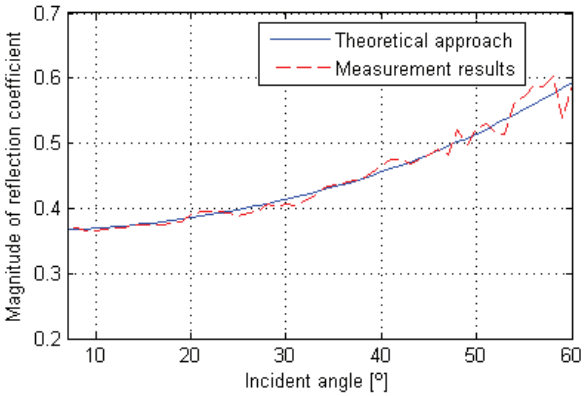

Fig. 7 – Measured and predicted reflection coefficient as function of incident angle for concrete slab with gravel [4-8mm], at 18.7GHz.

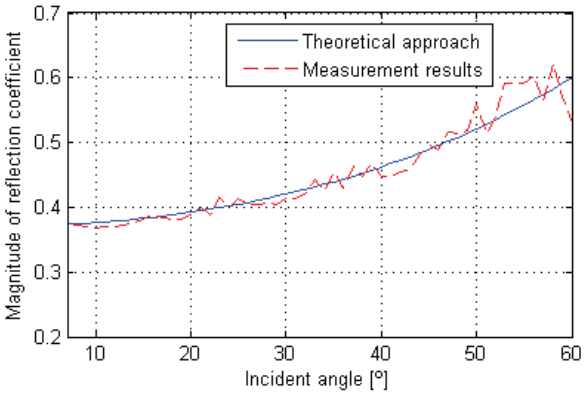

Fig. 8 – Measured and predicted reflection coefficient as function of incident angle for concrete slab with gravel [6-12mm], at 18.7GHz.

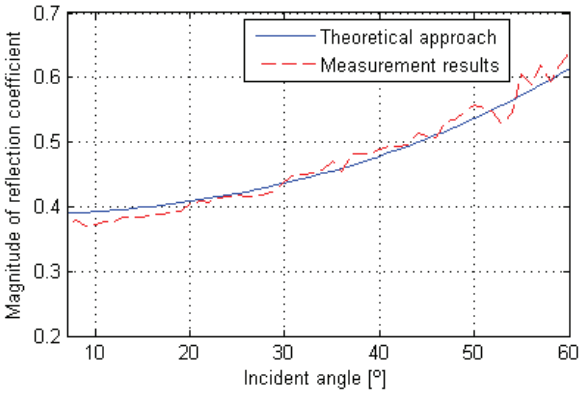

Fig. 9 – Measured and predicted reflection coefficient as function of incident angle for concrete slab with gravel [12-20mm], at 18.7GHz.

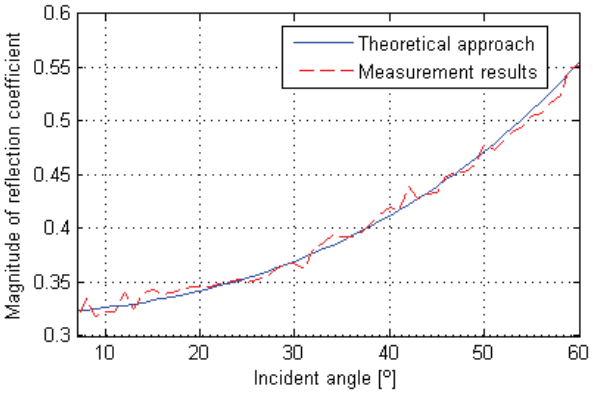

Fig. 10– Measured and predicted reflection coefficient as function of incident angle for concrete slab without gravel, at 60GHz.

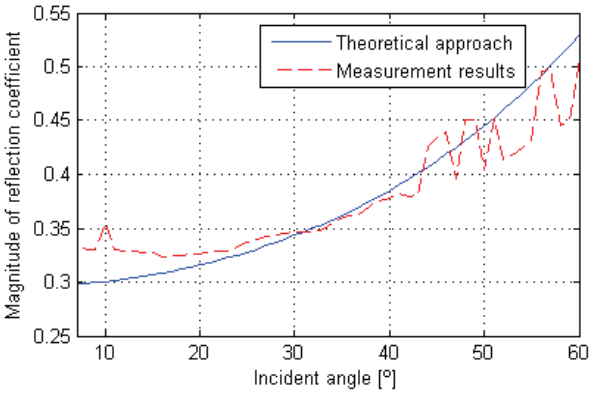

Fig. 11 – Measured and predicted reflection coefficient as function of incident angle for concrete slab with gravel [4-8mm], at 60GHz.

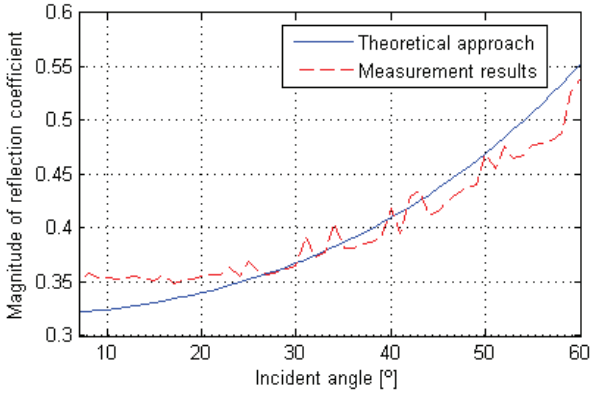

Fig. 12 – Measured and predicted reflection coefficient as function of incident angle for concrete slab with gravel [6-12mm], at 60GHz.

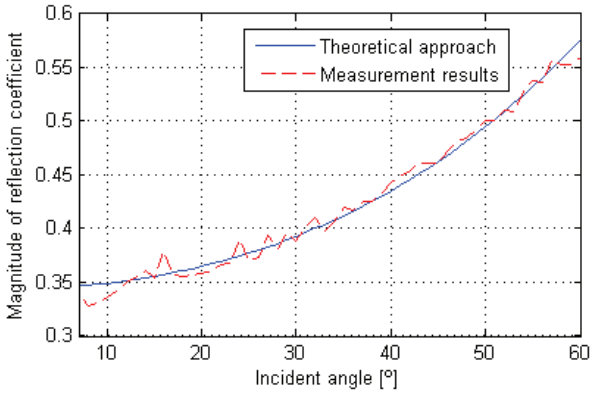

Fig. 13 – Measured and predicted reflection coefficient as function of incident angle for concrete slab with gravel [12-20mm], at 60GHz.

The dielectric parameters were found by fitting the reflection functions to theoretical ones with least RMSE criteria. A summary of the dielectric parameters obtained for all materials tested and RMS error are given in Table I for 18.7 GHz and Table II for 60 GHz.

TABLE I. AVERAGE DIELECTRIC PROPERTIES FOR DIFFERENT TYPES OF CONCRETE AT 18.7 GHZ

Material	Permittivity	Loss tangent	RMS error
Concrete without gravel	3.951	0.0998	0.126
Concrete with gravel (4 to 8 mm)	4.568	0.104	2.352e-5
Concrete with gravel (6 to 12 mm)	4.752	0.027	1.056e-5
Concrete with gravel (12 to 20 mm)	5.103	0.061	3.247e-5

TABLE II. AVERAGE DIELECTRIC PROPERTIES FOR DIFFERENT TYPES OF CONCRETE AT 60 GHZ

Material	Permittivity	Loss tangent	RMS error
Concrete without gravel	3.6487	0.2053	8.325e-5
Concrete with gravel (4 to 8 mm)	3.2878	0.175	1.435e-5
Concrete with gravel (6 to 12 mm)	3.713	0.114	9.988e-5
Concrete with gravel (12 to 20 mm)	4.149	0.114	3.768e-5

V. CONCLUSIONS

Reflection coefficients for various building materials were measured as a function of the incident angle at 18.7 and 60 GHz. It is shown that the multi-dielectric model describes these functions accurately, and therefore is suited to be used to estimate the dielectric parameters. These results provide useful information for propagation-related research in the development of various millimetre-wave application systems.

Further work will address the development of a model that characterises reflection coefficient dependence with the thickness of the gravel inside the concrete walls. In addition, other commonly used construction materials will also be measured and characterised. Finally, several multi-dielectric measurements, performed with combinations of elemental materials previously characterised, will also be performed and compared against the multi-dielectric theoretical model.

REFERENCES

[1] Feuerstein M.J., Landron O., and Rappaport T.S., “In situ microwave reflection coefficient measurements for smooth and rough exterior wall surfaces,” In Proceedings IEEE Vehicular Technology Conference, , no. 461, pp. 77–80, April 1999.

[2] Ana Vazquez Alejos, Measurement, Characterization and Modeling of the Radio Channel for Broadband Multimedia Systems at 40GHz, Ph.D. thesis, Universidade de Vigo, 2006.

[3] Hammoudeh A., Pugliese J.P., Sanchez M.G., and Grindrod E., “Comparison of reflection mechanisms from smooth and rough surfaces at 62GHz,” National Conference on Antennas and Propagation, pp. 77–80, May 1993.

[4] Balanis and Constantine A., Advanced Engineering Electromagnetics, John Willey & Sons, 1989.

[5] Sophocles J. Orfanidis” Electromagnetic Waves and Antennas”, ECE Department, Rutgers University, 2004.

[6] Landron, O. : Microwave Multipath Resolution in Microcellular Environments, Virginia Tech Masters Thesis. August 1992.

[7] O. Landron, M. J. Feuerstein and T. S. Rappaport, “In Situ Microwave Reflection Coefficient Measurements for Smooth and Rough Exterior Wall Surfaces”, 1993.